
ReXNet: Diminishing Representational Bottleneck on Convolutional Neural Network

Dongyoong Han Sangdoo Yun Byeongho Heo YoungJoon Yoo

Clova AI Research, NAVER Corp.

Abstract

This paper addresses representational bottleneck in a network and propose a set of design principles that improves model performance significantly. We argue that a representational bottleneck may happen in a network designed by a conventional design and results in degrading the model performance. To investigate the representational bottleneck, we study the matrix rank of the features generated by ten thousand random networks. We further study the entire layer’s channel configuration towards designing more accurate network architectures. Based on the investigation, we propose simple yet effective design principles to mitigate the representational bottleneck. Slight changes on baseline networks by following the principle leads to achieving remarkable performance improvements on ImageNet classification. Additionally, COCO object detection results and transfer learning results on several datasets provide other backups of the link between diminishing representational bottleneck of a network and improving performance. Code and pretrained models are available at <https://github.com/clovaai/rexnet>.

1 Introduction

Modeling efficient, so-called lightweight, networks is one of the most important issues in computer vision for both researchers and practitioners. Previously proposed efficient models [13, 41, 12, 48] have tried to find a *cheap* network design (e.g., shrinking channel dimension) by focusing on computational efficiency, showing promising trade-offs between the computational cost and accuracy.

In this paper, we aim to find out what network design principles followed by the above methods are missing, *representational bottleneck*. As a pioneer, [46] conceptually introduced the representational bottleneck caused by extreme compression of channel dimension. The authors regard a feed-forward network as an acyclic graph, and the information flow from the input to the output can be hampered by architectural design such as extreme compression. In language modeling, as a milestone work, [55] firstly revealed the existence of representational bottleneck at the softmax layer, *Softmax bottleneck*. The authors show the bounded matrix rank causes the representational bottleneck and handle this by expanding the rank with additional nonlinearity on the linear softmax. The successors [19, 7] also observed that the softmax layer’s low rank can cause the representational bottleneck which degrades the overall performance of the model.

Taking a further step from the above pioneering works, we investigate the representational bottleneck of the entire layers of a network. We first show there exist layers that are limited in the encoding capability of generating discriminative features considered as the representational bottleneck. We provide a simple theoretical backup using matrix rank analysis of intermediate features. Also, we conduct empirical studies to investigate the representational bottleneck through randomly generated networks and verify the matrix rank of weights is directly linked to the model’s performance. By the evidence, we propose a set of new design principles to boost the actual performance of the model: 1) enlarge the input channel size (dimension) of a layer; 2) equip with a proper nonlinearity; 3) design a network with many expand layers. We further train the network which is designed according to the

principles upon an existing network on ImageNet dataset [40] and compute the matrix rank of the layers to provide a practical backup.

Finally, we propose our new models **Rank eXpansion Networks** (ReXNets) following the design principles. It turns out that a simple modification upon the baseline models could show remarkable improvement in performance on ImageNet classification. Our models even outperform the state-of-the-art networks whose architectures were found by neural architecture search (NAS) that requires huge computational resources. Thus, this work will encourage the researchers in NAS field to adopt our simple yet effective design principles into their search space for further performance boosts. The performance improvement of the ImageNet classification is well transferred to the object detection on COCO dataset [25] and to the various fine-grained classification tasks, showing the effectiveness of our model as a strong feature extractor.

Our contributions are: investigation of representational bottleneck problem that happens in a network through a mathematical and an empirical studies (§2); new design principles with improved network architectures (§3); state-of-the-art results on ImageNet dataset [40] and prominent transfer learning results on COCO detection [25] and four different fine-grained classifications (§4).

2 On Representational Bottleneck

2.1 Preliminary: Feature encoding

Given an L -depth network, N features are encoded from d_0 -dimensional input $\mathbf{X}_0 \in \mathbb{R}^{d_0 \times N}$. Features are represented as $\mathbf{X}_L = \sigma(\mathbf{W}_L(\dots f_1(\mathbf{W}_1 \mathbf{X}_0)))$ with the weight matrix $\mathbf{W}_i \in \mathbb{R}^{d_i \times d_{i-1}}$. We call the layer with $d_i > d_{i-1}$ an *expand layer*, and the layer with $d_i < d_{i-1}$ an *condense layer*. Each of $f_i(\cdot)$ denotes i -th point-wise nonlinearity, such as a ReLU [33] with a Batch Normalization (BN) layer [18]. $\sigma(\cdot)$ denotes Softmax function. When training the network, every single forward step encodes an input \mathbf{X}_0 to the output \mathbf{X}_L to minimize the gap between \mathbf{X}_L and label matrix $\mathbf{T} \in \mathbb{R}^{d_L \times N}$. Therefore, how effectively the features are encoded towards the label is related to how well it is likely to reduce the gap. The formulation for a CNN is slightly changed to $\mathbf{X}_L = \sigma(\mathbf{W}_L * (\dots f_1(\mathbf{W}_1 * \mathbf{X}_0)))$, where $*$ and \mathbf{W}_i denote the convolution operation and the i -th convolutional layer's weight with kernel size k_i , respectively. We rewrite each convolution with the conventional reordering [3] by $\mathbf{W}_i \hat{\mathbf{X}}_{i-1}$, where $\mathbf{W}_i \in \mathbb{R}^{d_i \times k_i^2 d_{i-1}}$ and the reordered feature $\hat{\mathbf{X}}_{i-1} \in \mathbb{R}^{k_i^2 d_{i-1} \times whN}$. We write the i -th feature as

$$\mathbf{X}_i = \begin{cases} f_i(\mathbf{W}_i \hat{\mathbf{X}}_{i-1}) & 1 \leq i < L, \\ \sigma(\mathbf{W}_L \hat{\mathbf{X}}_{L-1}) & i = L. \end{cases} \quad (1)$$

2.2 Representational bottleneck and matrix rank

Revisiting Softmax bottleneck. We revisit Softmax bottleneck [55], a sort of representational bottleneck, happened at the softmax layer to formalize representational bottleneck. From eq.(1), the output of the cross-entropy loss is $\log \mathbf{X}_L = \log \sigma(\mathbf{W}_L \mathbf{X}_{L-1})$, whose rank is bounded by the rank of $\mathbf{W}_L \mathbf{X}_{L-1}$, which is $\min(d_L, d_{L-1})$. As the input dimension d_{L-1} is smaller than the output dimension d_L , the encoded features cannot fully represent the whole category due to the rank deficiency. This shows an instance of the representational bottleneck at a softmax layer. To resolve the issue, the related works [55, 19, 7] have shown large performance improvements by mitigating the rank deficiency of the softmax layer via involving non-linearity function. Furthermore, what if we increase d_{L-1} closer to d_L , does it become another solution to diminish the representational bottleneck? We will take a look at this in later sections.

Diminishing representational bottleneck by layer-wise rank expansion. Let us consider some popular networks [42, 9, 13, 41] designed for ImageNet classification task [40]. The networks are designed to have the output channels (before the classifier) up to 1,000 using downsampling blocks by doubling the input channel size, while leaving the other layers with the same output and input channel sizes. We conjecture the layers that expand the channel size (i.e., expand layers) such as downsampling blocks would have a rank deficiency and may have the representational bottleneck.

Our goal is to mitigate the representational bottleneck problem in the intermediate layers by expanding the rank of weight matrix \mathbf{W}_i . Given the i -th feature generated by a layer, $\mathbf{X}_i = f_i(\mathbf{W}_i \mathbf{X}_{i-1}) \in$

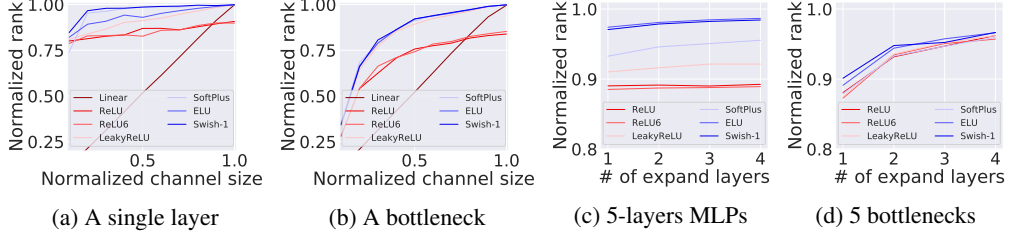


Figure 1: **Normalized rank of networks.** The normalized rank (i.e., rank/output channel size) vs. normalized channel size (i.e., input channel size/output channel size) is computed from the feature of (a) single layer networks and (b) networks with a bottleneck block, respectively and averaged over 10,000 randomly generated networks. Furthermore, we study the channel size configuration of the entire layers of the networks with (c) 5-layer MLPs and (d) 5-bottleneck blocks. We average the normalized rank of 10,000 randomly generated networks with respect to the number of expand layers.

Table 1: **Accuracy and the number of expand layers.** We train four networks sampled from each configuration of different number of expand layers on CIFAR100 dataset [23]. We average the results over 5 networks due to the random initialization. Norm. Rank denotes the averaged normalized rank of randomly generated networks.

# of exp. layers	Channel Conf. (%)	Top-1 acc. (%)	Norm. Rank	Params. (M)
1	32-100-100-100	61.90	0.87	0.14
2	32-64-120-120	62.08	0.93	0.16
3	32-64-112-112-128	62.10	0.95	0.15
4	32-90-100-110-120	62.15	0.96	0.15

$\mathbb{R}^{d_i \times wh^N}$, $\text{rank}(\mathbf{X}_i)$ is bounded to $\min(d_i, d_{i-1})$ (we assume $N \gg d_i$). We represent $f(\mathbf{X}) = \mathbf{X} \circ g(\mathbf{X})$, where \circ denotes the pointwise multiplication with another pointwise function g . Following the inequality $\text{rank}(f(\mathbf{X})) \leq \text{rank}(\mathbf{X}) \cdot \text{rank}(g(\mathbf{X}))$ [32], the rank of feature \mathbf{X}_i is bounded as,

$$\text{rank}(\mathbf{X}_i) \leq \text{rank}(\mathbf{W}_i \mathbf{X}_{i-1}) \cdot \text{rank}(g_i(\mathbf{W}_i \mathbf{X}_{i-1})). \quad (2)$$

Therefore, we conclude the rank bound can be expanded by increasing $\text{rank}(\mathbf{W}_i \mathbf{X}_{i-1})$ and replacing with a proper function g_i that has a larger rank such as using Swish-1 [36] or ELU [4], which is similarly done in the work [55]. When d_i is fixed, if we adjust the feature dimension d_{i-1} close to d_i , eq.(2) provides the possibility of the unbounded rank up to the feature dimension. For a bottleneck block [9, 41] consists of consecutive 1×1 , 3×3 , and 1×1 convolutions, we identically expand the rank bound by eq.(2) by considering the input and output channel sizes of a bottleneck block¹.

2.3 Empirical study

In this section, we conduct two empirical studies: layer-level analysis and the entire layer’s channel configuration study using the matrix rank. First, we empirically investigate how the matrix rank of a layer is actually expanded. This study aims to how the input channel size d_i and the following nonlinearity (f_i) affect the matrix rank, as we have discussed in §2.2. To this end, we design experiments for a single layer and a bottleneck using a large number of networks ($>10,000$ networks) whose building components (e.g., channel size, or non-linearity function) are randomly sampled and measure the rank of them. Second, based on the layer-level study, we investigate the whole channel configuration of a network by measuring the matrix rank and the real performance of the network to find a better network architecture. Using fixed-depth random networks again, we make a connection between the measured ranks and real model performances. This leads us to provide design principles for a network with expanded rank, eventually improving actual performance.

Layer-level rank analysis. To do layer-level rank analysis, we generate a set of random networks consist of a single layer: $f(\mathbf{WX})$ with $\mathbf{W} \in \mathbb{R}^{d_{out} \times d_{in}}$ and $\mathbf{X} \in \mathbb{R}^{d_{in} \times N}$, where d_{out} is randomly

¹ Consider the feature generated by a bottleneck block, which is represented as $\mathbf{Y} = f_a(\mathbf{W}_a f_b(\mathbf{W}_b \hat{\mathbf{X}}_c))$ with two weights $\mathbf{W}_a \in \mathbb{R}^{d_{out} \times d_m}$ and $\mathbf{W}_b \in \mathbb{R}^{d_m \times k^2 d_n}$, where $\hat{\mathbf{X}}_c \in \mathbb{R}^{k^2 d_n \times d_m}$ is the reordered feature of $f_c(\mathbf{W}_c \mathbf{X})$. Then, $\text{rank}(\mathbf{Y}) = \min(\text{rank}(\mathbf{W}_a \mathbf{W}_b), \text{rank}(\hat{\mathbf{X}}_c)) = \min(\min(d_{out}, d_m, k^2 d_n), k^2 d_n, d_m) = \min(d_{out}, d_m, k^2 d_n, d_m)$. ResNet [9] and MobileNetV2 [41] adjusted $d_m = d_n = \rho d_{in}$, where ρ denotes the expansion ratio 0.25 and 6, respectively. Finally, we have $\text{rank}(\mathbf{Y}) = \min(d_{out}, d_{in})$ for inverted bottleneck [41] and $\text{rank}(\mathbf{Y}) = \min(d_{out}, \rho d_{in})$ for bottleneck block [9]. In any cases, we can expand the rank bound by increasing d_{in} close to d_{out} .

sampled, and d_{in} is proportionally adjusted. We measure the normalized rank from the features ($\text{rank}(f(\mathbf{W}\mathbf{X}))/d_{out}$) produced by each network. To investigate f , widely-used nonlinear functions² are considered. We repeat the experiment for 10,000 networks for each normalized channel size (d_{in}/d_{out}) in $[0.1, 1.0]$ and for each nonlinearity. A bottleneck block [9, 41] is similarly studied by generating three consecutive random layers (i.e., by decomposing \mathbf{W} into three matrices with arbitrary sizes). The inner expansion ratio of each bottleneck block is randomly set as well for generality. We report the normalized ranks in Figures 1a and 1b, which are averaged over 10,000 networks for a single layer and a bottleneck block, respectively.

Channel configuration study. We now consider how to design a network of assigning the channel size of the entire layers. We randomly generate L -depth networks with expand layers (i.e., $d_{out} > d_{in}$) and the layers with $d_{out} = d_{in}$ following the design trend using few condense layers because a condense layer directly reduces the model capacity [46]. We change the number of expand layers from 0 to $L - 1$ and generate networks randomly. For example, a network with the number of expand layers is 0, all the layer has the same channel size (except for the channel size of the stem layer). We repeat the experiments with each randomly generated 10,000 networks and average the normalized rank. The results are shown in Figures 1c and 1d. Additionally, we report the actual performance of the sampled networks that have 5 bottlenecks with the stem channel size of 32 for each configuration with a different number of expand layers. We train the networks on CIFAR100 dataset [23] and report the accuracy averaged over 5 networks (due to the random initialization of weights) in Table 1.

Observations. From Figures 1a and 1b, we observe properly selected nonlinear functions can largely expand the rank comparing to the linear case. Second, the normalized input channel size (d_{in}/d_{out}) is closely related to the rank of the feature for both single layer (Figure 1a) and bottleneck block (Figure 1b) cases. For the entire layer’s channel configuration, Figures 1c and 1d show that the rank can be expanded using more expand layers when the network depth is fixed. Furthermore, this rank trend is well matched to the actual performance as shown in Table 1. The observations give the design principles that expand the rank of a given network: 1) expand the input channel size d_{in} at a layer; 2) find a proper nonlinearity; 3) a network should be designed with many expand layers.

3 Improved Network Architecture

3.1 Where does representational bottleneck occur?

We now consider which layer the representation bottleneck may occur in a network. All popular deep networks have a similar architecture with many expand layers to expand channels from 3-channel input to c -channel output prediction for image sources. First, downsampling blocks [9, 41] or layers [42] is performed like an expand layer. Second, the first layer in a bottleneck module [9, 10, 53] and inverted bottleneck blocks [41, 12, 47] is an expand layer as well. Finally, there exists the penultimate layer that largely expands output channel size. We claim that the representational bottleneck would happen at these expand layers and the penultimate layer.

3.2 Network Redesign

Intermediate convolutional layers. We first consider MobileNetV1 [13]. We sequentially make the same modifications on convolutions, closer to the penultimate layer. We refine each layer by 1) expanding the input channel size of the convolution layer and 2) replacing the ReLU6s. Second, we renovate MobileNetV2 [41] similarly in MobileNetV1. All the inverted bottlenecks from the end to the first are sequentially modified by the same principle. How much to expand the input channel size is an open question and would be managed by a NAS method, but for simplicity, we suggest instance models of following our design principles in the supplementary material. Note that we can also renovate popular networks such as ResNet [9] or VGG [42]. In ResNet and its variants [9, 10, 53], there is no nonlinearity after the third convolutional layer in each bottleneck block, so expanding the input channel size is the only remedy. We show how expanding the input channel size on ResNet and further on VGG can improve the performance in §5.2.

The penultimate layer. The network architectures [9, 10, 16, 13, 41, 12, 47] have the convolutional layer with a relatively large output channel size at the penultimate layer. This was to prevent the representational bottleneck at the final classifier, but the penultimate layer still suffers from the problem. We expand the input channel size of the penultimate layer and replace the ReLU6.

²ReLU [33], ReLU6 [41], ELU [4], SoftPlus [6], LeakyReLU [30], and Swish-1 [36]

Table 2: **Model comparison with ReXNets on ImageNet.** We compare the classification results of ReXNet (1.0x) with popular lightweight models including the models searched by NAS methods (left) on ImageNet dataset [40]. We report ReXNets’ performances with different width multipliers (right) and compare with those of EfficientNets [48]. Note that ReXNets are trained and evaluated with the fixed image size 224×224 .

Network	Top-1 (%)		Top-5 (%)		FLOPs	Params.
MobileNetV1 [13]	70.6	89.5	0.575B	4.2M		
MobileNetV2 [41]	72.0	91.0	0.300B	3.5M		
CondenseNet [15]	73.8	91.7	0.529B	4.8M		
ShuffleNetV1 (x2) [57]	73.7	-	0.524B	-		
ShuffleNetV2 (x2) [29]	75.4	-	0.597B	-		
Pelee [51]	72.6	90.6	0.508B	2.8M		
NASNet-A [58]	74.0	91.7	0.564B	5.3M		
AmoebaNet-A [37]	75.5	92.0	0.555B	5.1M		
PNASNet [26]	74.2	91.9	0.588B	5.1M		
DARTS [27]	73.1	91.0	0.595B	4.9M		
FBNet-C [52]	74.9	-	0.375B	5.5M		
ProxylessNas [2]	74.6	93.3	0.320B	4.1M		
RandWire-WS [54]	74.7	92.2	0.583B	5.6M		
MnasNet-A3 [47]	76.7	32.3	0.403B	5.2M		
MobileNetV3-Large [12]	75.2	-	0.217B	5.4M		
FBNetV2-L1 [50]	77.2	-	0.325B	-		
EfficientNet-B0 [48]	77.3	93.5	0.399B	5.3M		
ReXNet-1.0x	77.9	93.9	0.398B	4.8M		
Network	Top-1 (%)		Top-5 (%)		FLOPs	Params.
ReXNet-plain	74.8	91.93	0.564B	3.41M		
ReXNet-0.9x	77.2	93.5	0.347B	4.1M		
ReXNet-1.0x	77.9	93.9	0.398B	4.8M		
EfficientNetB0 [48]	77.3	93.5	0.40B	5.3M		
ReXNet-1.1x	78.6	94.1	0.480B	5.6M		
ReXNet-1.2x	79.0	94.3	0.567B	6.6M		
ReXNet-1.3x	79.5	94.7	0.662B	7.6M		
EfficientNetB1 [48]	79.2	94.5	0.70B	7.8M		
ReXNet-1.4x	79.8	94.9	0.762B	8.6M		
ReXNet-1.5x	80.3	95.2	0.875B	9.7M		
EfficientNetB2 [48]	80.3	95.0	1.0B	9.2M		
ReXNet-2.0x	81.6	95.7	1.53B	16M		
ReXNet-2.2x	81.7	95.8	1.84B	19M		
EfficientNetB3 [48]	81.7	95.6	1.8B	12M		

(a) **Comparison of ImageNet top-1 accuracy.** All the accuracies are borrowed from the original papers.

(b) **ReXNets and EfficientNets.** Our models are compared with EfficientNets [48] on ImageNet.

ReXNets. We now introduce our models called **R**ank **e**xpansion **N**euroworks (ReXNets) following the design principles inspired by our investigation. We call ReXNet-plain and ReXNet, which are renovated upon MobileNetV1 [13] and MobileNetV2 [41], respectively. Note that our models are instances that show how diminishing the representational bottleneck affects the overall performance, which will be shown in the experiment section. Our design of channel configuration is roughly found to meet the overall parameters and flops of the baselines for fair comparison, so the better network architecture will be found by proper parameter searching methods such as NAS methods. The detailed model information is available in the supplementary material.

4 Experiment

4.1 ImageNet Classification

Training setup. We train our model on ImageNet dataset [40] with the fixed image size 224×224 . We use the standard data augmentation [45] with the random-crop rate from 0.08 to 1.0. Our models are trained using stochastic gradient descent (SGD) with Nesterov momentum [34] with momentum of 0.9 and mini-batch size of 512 with 4 GPUs. Learning rate is initially set to 0.5 and is linearly warmed up in the first 5 epochs following the method [8] then is decayed by the cosine learning rate scheduling. Weight decay is set to $1e-5$. We verify the correctness of our training setup by training MobileNetV1 and MobileNetV2. We achieve 72.5% and 73.1% that outperforms the reported scores 70.6% and 72.0%, respectively. See supplementary material for detailed training setup.

Our trained models. Here, we show our models: ReXNet-plain and ReXNet. We first train our models following the training setup on ImageNet from scratch using fixed image size. Furthermore, to show our models’ scalability, the simple width multiplier concept in the previous works [13, 41, 57, 29, 47, 12] is adopted to adjust the model size. As shown in Table 2b, our models are well scaled up to 2.2x from 0.9x with remarkable performances just using width multiplier.

Performance comparison. Table 2a shows the performance comparison with popular lightweight models. Note that all the models are trained and evaluated with 224×224 resolution images. Our models show significant performance improvements over the baselines, so our models can be compared with the models searched by NAS methods. Interestingly, our models could outperform EfficientNet-B0 and B1 [48], which are searched by NAS with comparable model size and FLOPs.

Table 3: **Object detection results on COCO test-dev 2017**. We report ReXNets in SSDLite to compare with both lightweight (FLOPs \simeq 1.0B) and heavier models (FLOPs $>$ 1.0B). We choose ReXNet-0.9x, 1.0x, and 1.3x for the feature extractor to compare with lightweight detectors, respectively. † : the model performances are trained by ourselves.

Model	Input Size	Avg. Precision at IOU (%)			Params.	FLOPs
		AP	AP ₅₀	AP ₇₅		
Pelee [51]	304x304	22.4	38.3	22.9	6.0M	1.29B
Tiny-DSOD [24]	300x300	23.2	40.4	22.8	1.2M	1.12B
MobileNetV1 [13] + SSDLite	320x320	22.2	-	-	5.1M	1.31B
MobileNetV2 [41] + SSDLite	320x320	22.1	-	-	4.3M	0.79B
MobileNetV3 [12] + SSDLite	320x320	22.0	-	-	5.0M	0.62B
MnasNet-A1 [47] + SSDLite	320x320	23.0	-	-	4.9M	0.84B
EfficientNetB0 [48] + SSDLite †	320x320	23.5	39.9	23.5	6.2M	0.97B
ReXNet-0.9x + SSDLite	320x320	24.4	41.1	24.7	5.0M	0.88B
ReXNet-1.0x + SSDLite	320x320	24.8	41.8	25.0	5.7M	1.01B
YOLOv3-tiny [39]	416x416	-	33.1	-	12.3M	5.56B
SSD [28]	300x300	23.2	41.2	23.4	36.1M	35.2B
SSD [28]	512x512	26.8	46.5	27.8	36.1M	99.5B
YOLOv2 [38]	416x416	21.6	44.0	19.2	50.7M	17.5B
EfficientNetB1 [48] + SSDLite †	320x320	25.7	43.0	26.1	8.7M	1.35B
EfficientNetB2 [48] + SSDLite †	320x320	26.0	43.2	26.4	10.0M	1.55B
ReXNet-1.3x + SSDLite	320x320	26.5	44.0	26.9	8.4M	1.60B

4.2 COCO Object Detection

Architecture details. We choose SSDLite [41] which is a lightweight detector that is suitable for viewing the feature extractor’s capability. We put the first head of SSDLite to the last feature extractor layer that has an output stride of 16 and put the second head to the last feature extractor layer that has an output stride of 32 by following [41, 12, 47]. This is to use the same size of the extracted features fairly because the detection performance is sensitive to the features’ resolution.

Performance comparison. We compare our models with popular lightweight detectors including SSD [28], SSDLites [13, 41, 12, 47], YOLOv2 [38], YOLOv3 [39], Pelee [51], and Tiny-DSOD [24]. Additionally, we report the detection performances of EfficientNets-B0, B1, and B2 as backbones in SSDLite. As shown in Table 3, ours largely outperform the performance of the other detectors with similar model sizes and FLOPs. Interestingly, as compared with the models using SSDLite, ours achieve much better performances. It is worth noting that ours outperforms EfficientNets-B1 and B2 with SSDLite, in which backbones are pretrained with larger image sizes (>224). We believe that this reflects diminishing the performance bottleneck would help a finetuning task as well.

Training setup. Our models are trained using stochastic gradient descent (SGD) with 1 GPU. We use the same setting of the previous works [41, 12, 47] including the input size of 320×320 and data augmentations. Learning rate is initially set to 0.05, and weight decay is set to 4e-5. Following the standard setting [28, 13, 41, 12, 47], we train the models on `train` 2017 and further evaluate on `test-dev` 2017 set at COCO test server. All the models except for Tiny-DSOD are finetuned using their own pretrained backbone.

4.3 Transfer learning with ReXNets

Training setup and performance comparison. We finetune our models on several datasets including Food-101 [1], Stanford Cars [22], FGVC Aircraft [31], and Oxford Flowers-102 [35]. We compare our models with the best performing models ResNet50 [9] and EfficientNet-B0 [48]. We exhaustively search the hyper-parameters including learning rate and weight decay for the best results for all the models like [21] for a fair comparison. We do not put additional techniques but training all the layers using SGD with Nesterov momentum. For all the datasets, training and evaluation are done with 224×224 image size, and we use center-cropped images of the same size after resizing images with the shorter side of 256 for evaluation. Note that we do not use larger image sizes such as 600×600 as in the work [48]. As shown in Table 4, ours outperform EfficientNet-B0 for all the datasets with large margins. Ours beat ResNet50 which has more than parameters (x5) on all the datasets except for Stanford Cars dataset. This indicates that our models have fewer parameters but perform as prominent feature extractors for transfer learning over other models.

Table 4: **Transfer learning results on four datasets.** We report transfer learning results on four fine-grained datasets including Food-101, Standford Cars, FGVC Aircraft, and Oxford Flower-102. All the Top-1 scores of the models are reported by training and testing with 224×224 image size.

Dataset	Network	Top-1 acc. (%)	FLOPs	Params.
Food-101 [1]	ResNet50 [9]	87.03	4.1B	25.6M
	EfficientNet-B0 [48]	87.47	0.4B	5.3M
	ReXNet-1.0x	88.41	0.4B	4.8M
Stanford Cars [22]	ResNet50 [9]	92.58	4.1B	25.6M
	EfficientNet-B0 [48]	90.66	0.4B	5.3M
	ReXNet-1.0x	91.45	0.4B	4.8M
FGVC Aircraft [31]	ResNet50 [9]	89.42	4.1B	25.6M
	EfficientNet-B0 [48]	87.06	0.4B	5.3M
	ReXNet-1.0x	89.52	0.4B	4.8M
Oxford Flowers-102 [35]	ResNet50 [9]	97.72	4.1B	25.6M
	EfficientNet-B0 [48]	97.33	0.4B	5.3M
	ReXNet-1.0x	97.82	0.4B	4.8M

5 Ablation Study and Discussion

5.1 Ablation studies

Impact on replacing nonlinearities. We study the impacts of replacing 1) the first nonlinearity in each inverted bottleneck, and 2) the last nonlinearity at the penultimate layer. Both of them are after expand layers, we expected that the performance is improved as they are replaced. As shown in Table 5a, the first nonlinearity affects more on the performance than the second one does. First, Table 5c shows that both of the nonlinearities affect the performance when they are replaced. In MobileNetV1, Table 5d shows a similar trend, but the second nonlinearity also affect a little. We hypothesis this is because MobileNetV1 needs additional model capacity.

Impact on expanding channel size. We study how expanding the output channel size of the input feature work together with replacing the nonlinearity. As shown in Table 5c, it works well together with replacing the nonlinearities. MobileNetV1 result in Table 5d show similar result as well.

5.2 Discussions

ReX-ResNet and ReX-VGG. We apply our principles to ResNet and VGG. We choose ResNet50 [9] and VGG16-BN [42]. We found the accuracy improvements on ResNet50 (77.1% (ours) vs 76.3%) and on VGG16-BN (71.8% (ours) vs. 71.6%) on ImageNet, while with similar computational costs.

Verifying representational bottleneck in pretrained models. We now make a final backup by measuring the matrix rank of the output of each layer to reveal the representational bottleneck. Specifically, we use two ImageNet-trained models (MobileNetV2 and a renovated MobileNetV2 that follows our design principles) to visualize the cumulative distribution of the singular values computed with each feature set. Using randomly sampled 2,000 images in ImageNet validation set, we compute the singular values from the extracted features of 1) each layer after the nonlinearity in every inverted bottleneck and 2) after the nonlinearity at the penultimate layer. We first normalize all singular values to $[0, 1]$ to manage different singular values from different layers and then plot the cumulative percentage of normalized singular values for each layer. As shown in Figure 2, many

Table 5: **Ablation study of rank expansion and nonlinearity.** From (a) to (c), “1st act.” and “2nd act.” denote the first and the second ReLU6 in each bottleneck block, respectively, and “Pen act.” denotes the ReLU6 that follows the penultimate layer in MobileNetV2. For (d), “1st act.” and “2nd act.” denote the activation after 1×1 convolution and 3×3 depthwise convolution in MobileNetV1. “Exp.” denotes the model consists of expand layers by increasing the input channel size of each layer.

1st act. 2nd act. Top-1 Top-5	1st act. Pen. act. Top-1 Top-5	Exp. 1st act. Pen. act. Top-1 Top-5	Exp. 1st act. 2st act. Top-1 Top-5
- - 73.08 91.28	- - 73.08 91.28	- - - 73.08 91.28	- - - 72.56 90.67
- ✓ 73.34 91.33	✓ - 73.59 91.59	✓ - - 75.45 92.60	✓ - - 73.64 91.41
✓ ✓ 73.67 91.56	- ✓ 73.49 91.41	✓ ✓ - 75.65 92.83	✓ ✓ - 74.11 91.73
✓ - 73.59 91.59	✓ ✓ 73.95 91.46	✓ ✓ ✓ 75.86 92.86	✓ ✓ ✓ 74.21 91.76

(a) **On nonlinearities** in MobileNetV2 (b) **On nonlinearities** in MobileNetV2 (c) **On rank expansion and nonlinearities** in MobileNetV2 (d) **On rank expansion and nonlinearities** in MobileNetV1

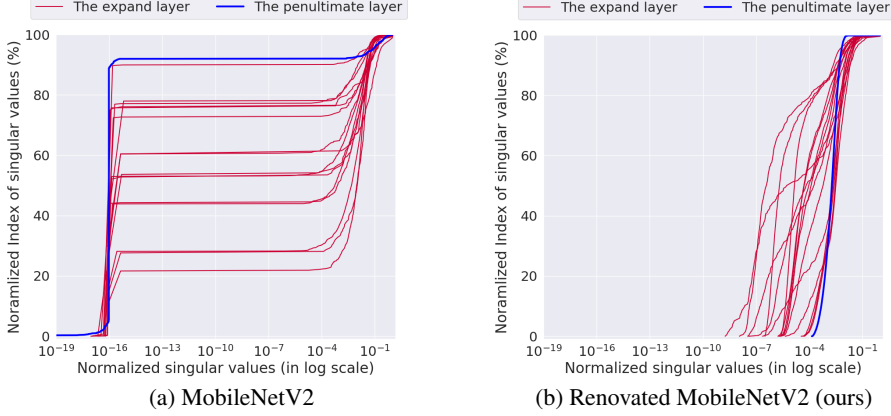


Figure 2: **Visualization of singular values.** We compute the cumulative sum of the singular values for all the expand layers in MobileNetV2 and ours trained on ImageNet.

Table 6: **Correlation between backbone and finetuning performance.** We study the correlation between the top-1 classification accuracy of backbones on ImageNet (ImageNet Top-1 Acc.) and the corresponding average precision on COCO (COCO AP). We observe a better backbone in respect to the ImageNet performance does not always link to the detection performance. However, ReXNet’s detection performance has improved to match the performance improvement of the backbone without excessive computational costs.

Backbone	Detector	ImageNet Top-1 Acc. (%)	COCO AP	Params.	FLOPs
MobileNetV1 [13]	SSDLite	70.6	22.2	5.1M	1.31B
MobileNetV2 [41]	SSDLite	72.0	22.1	4.3M	0.79B
MobileNetV3-Large [12]	SSDLite	75.2	22.0	5.0M	0.62B
MnasNet-A1 [47]	SSDLite	75.2	23.0	4.9M	0.84B
EfficientNetB0 [48]	SSDLite	77.3	23.5	6.2M	0.97B
ReXNet-0.9x	SSDLite	77.2	24.4	5.0M	0.88B

singular values from the layers are extremely low for MobileNetV2 compared with those of ours. This indicates our model has successfully overcome the representational bottleneck at layers.

Representational bottleneck and finetuning. We argue that increasing the classification accuracy may not link to the finetuning performance improvement. As shown in Table 6, MnasNet and MobileNetV3-Large are the first instances, where they have similar ImageNet accuracy but COCO APs are different. Second, when comparing MobileNetV1 and MobileNetV2 with MobileNetV3-Large, there is a large gap ImageNet accuracy, but not much in COCO AP. Also, EfficientNetB0 show higher classification accuracy than ReXNet-0.9x about 0.1%, but show inferior COCO AP about 1.0%. Through this result, we believe that a backbone when diminishing representational bottleneck is likely to have better encoding capacity inducing a better performance on a finetuning task.

ImageNet accuracy with different nonlinear functions. We further train ReXNet-x1.0 with ELU [4], SoftPlus [6], LeakyReLU [30], and ReLU6 [41] to compare with the model with Swish-1 [36]. This is to see the actual quality of the nonlinearities along with the study in Figure 1. We obtain the results of top-1 accuracy which is better in the order of Swish-1 (77.90%), ELU (77.64%), SoftPlus (77.60%), Leaky ReLU (77.44%), and ReLU6 (77.26%) (see supplementary material).

6 Conclusion

In this work, we have addressed *representational bottleneck* in CNN layers. Motivated by the representational bottleneck in language modeling, we hypothesized a similar representational bottleneck in the layers of a CNN. We further argued that the matrix rank is closely related to the bottleneck problem, and the model performance will be improved by diminishing it. We have proposed an experimental study that *expand layers* are likely to suffer from the representational bottleneck, so we propose a set of design principles to handle the problem. In the end, we achieved the models that successfully manage the problem, and the secured models that have renovated by following the principles outperformed the recent competitive models, including NAS-based models on ImageNet dataset. Furthermore, our models even showed the remarkable finetuning performances on COCO object detection and on several fine-grained datasets for transfer learning. Consequently, we believe that our work highlighted a new perspective of designing a network for many tasks.

Acknowledgement

We would like to thank Clova AI Research team members including Junsuk Choe, Seong Joon Oh, Sanghyuk Chun for fruitful discussions and internal reviews. In particular, we would like to thank Jung-Woo Ha who suggested the name of our network architecture. Naver Smart Machine Learning (NSML) platform [20] has been used in the experiments.

References

- [1] L. Bossard, M. Guillaumin, and L. Van Gool. Food-101—mining discriminative components with random forests. In *European conference on computer vision*, pages 446–461. Springer, 2014.
- [2] H. Cai, L. Zhu, and S. Han. Proxylessnas: Direct neural architecture search on target task and hardware. In *ICLR*, 2018.
- [3] S. Chetlur, C. Woolley, P. Vandermersch, J. Cohen, J. Tran, B. Catanzaro, and E. Shelhamer. cudnn: Efficient primitives for deep learning. *arXiv preprint arXiv:1410.0759*, 2014.
- [4] D.-A. Clevert, T. Unterthiner, and S. Hochreiter. Fast and accurate deep network learning by exponential linear units (elus). In *ICLR*, 2016.
- [5] E. D. Cubuk, B. Zoph, J. Shlens, and Q. V. Le. Randaugment: Practical data augmentation with no separate search. *arXiv preprint arXiv:1909.13719*, 2019.
- [6] C. Dugas, Y. Bengio, F. Bélisle, C. Nadeau, and R. Garcia. Incorporating second-order functional knowledge for better option pricing. In *NIPS*, 2001.
- [7] O. Ganea, S. Gelly, G. Becigneul, and A. Severyn. Breaking the softmax bottleneck via learnable monotonic pointwise non-linearities. In *ICML*, 2019.
- [8] P. Goyal, P. Dollár, R. Girshick, P. Noordhuis, L. Wesolowski, A. Kyrola, A. Tulloch, Y. Jia, and K. He. Accurate, large minibatch sgd: Training imagenet in 1 hour. *arXiv preprint arXiv:1706.02677*, 2017.
- [9] K. He, X. Zhang, S. Ren, and J. Sun. Deep residual learning for image recognition. In *CVPR*, 2016.
- [10] K. He, X. Zhang, S. Ren, and J. Sun. Identity mappings in deep residual networks. In *ECCV*, 2016.
- [11] A. Hermans, L. Beyer, and B. Leibe. In defense of the triplet loss for person re-identification. *arXiv preprint arXiv:1703.07737*, 2017.
- [12] A. Howard, M. Sandler, G. Chu, L.-C. Chen, B. Chen, M. Tan, W. Wang, Y. Zhu, R. Pang, V. Vasudevan, et al. Searching for mobilenetv3. In *ICCV*, 2019.
- [13] A. G. Howard, M. Zhu, B. Chen, D. Kalenichenko, W. Wang, T. Weyand, M. Andreetto, and H. Adam. Mobilenets: Efficient convolutional neural networks for mobile vision applications. *arXiv preprint arXiv:1704.04861*, 2017.
- [14] J. Hu, L. Shen, and G. Sun. Squeeze-and-excitation networks. In *arXiv:1709.01507*, 2017.
- [15] G. Huang, S. Liu, L. Van der Maaten, and K. Q. Weinberger. Condensenet: An efficient densenet using learned group convolutions. In *CVPR*, 2018.
- [16] G. Huang, Z. Liu, and K. Q. Weinberger. Densely connected convolutional networks. In *CVPR*, 2017.
- [17] G. Huang, Y. Sun, Z. Liu, D. Sedra, and K. Weinberger. Deep networks with stochastic depth. In *ECCV*, 2016.
- [18] S. Ioffe and C. Szegedy. Batch normalization: Accelerating deep network training by reducing internal covariate shift. In *ICML*, 2015.
- [19] S. Kanai, Y. Fujiwara, Y. Yamanaka, and S. Adachi. Sigsoftmax: reanalysis of the softmax bottleneck. In *NIPS*, 2018.
- [20] H. Kim, M. Kim, D. Seo, J. Kim, H. Park, S. Park, H. Jo, K. Kim, Y. Yang, Y. Kim, et al. NSML: Meet the MLaaS platform with a real-world case study. *arXiv preprint arXiv:1810.09957*, 2018.
- [21] S. Kornblith, J. Shlens, and Q. V. Le. Do better imagenet models transfer better? In *Proceedings of the IEEE conference on computer vision and pattern recognition*, pages 2661–2671, 2019.
- [22] J. Krause, J. Deng, M. Stark, and L. Fei-Fei. Collecting a large-scale dataset of fine-grained cars. In *Second Workshop on Fine-Grained Visual Categorization*, 2013.
- [23] A. Krizhevsky. Learning multiple layers of features from tiny images. In *Tech Report*, 2009.
- [24] Y. Li, J. Li, W. Lin, and J. Li. Tiny-dsod: Lightweight object detection for resource-restricted usages. In *BMVC*, 2018.
- [25] T.-Y. Lin, M. Maire, S. Belongie, J. Hays, P. Perona, D. Ramanan, P. Dollár, and C. L. Zitnick. Microsoft coco: Common objects in context. In *ECCV*, 2014.

[26] C. Liu, B. Zoph, M. Neumann, J. Shlens, W. Hua, L.-J. Li, L. Fei-Fei, A. Yuille, J. Huang, and K. Murphy. Progressive neural architecture search. In *ECCV*, 2018.

[27] H. Liu, K. Simonyan, and Y. Yang. Darts: Differentiable architecture search. *ICLR*, 2019.

[28] W. Liu, D. Anguelov, D. Erhan, C. Szegedy, S. Reed, C.-Y. Fu, and A. C. Berg. Ssd: Single shot multibox detector. In *ECCV*, 2016.

[29] N. Ma, X. Zhang, H.-T. Zheng, and J. Sun. Shufflenet v2: Practical guidelines for efficient cnn architecture design. In *ECCV*, 2018.

[30] A. L. Maas, A. Y. Hannun, and A. Y. Ng. Rectifier nonlinearities improve neural network acoustic models. In *ICML Workshop on Deep Learning for Audio, Speech and Language Processing*, 2013.

[31] S. Maji, E. Rahtu, J. Kannala, M. Blaschko, and A. Vedaldi. Fine-grained visual classification of aircraft. *arXiv preprint arXiv:1306.5151*, 2013.

[32] E. Million. The hadamard product. 2007.

[33] V. Nair and G. E. Hinton. Rectified linear units improve restricted boltzmann machines. In *ICML*, 2010.

[34] Y. E. Nesterov. A method for solving the convex programming problem with convergence rate $\mathcal{O}(1/k^2)$. *Dokl. Akad. Nauk SSSR*, 269:543–547, 1983.

[35] M.-E. Nilsback and A. Zisserman. Automated flower classification over a large number of classes. In *2008 Sixth Indian Conference on Computer Vision, Graphics & Image Processing*, pages 722–729. IEEE, 2008.

[36] P. Ramachandran, B. Zoph, and Q. V. Le. Searching for activation functions. *arXiv preprint arXiv:1710.05941*, 2017.

[37] E. Real, A. Aggarwal, Y. Huang, and Q. V. Le. Regularized evolution for image classifier architecture search. In *AAAI*, 2019.

[38] J. Redmon and A. Farhadi. Yolo9000: better, faster, stronger. In *CVPR*, 2017.

[39] J. Redmon and A. Farhadi. Yolov3: An incremental improvement. *arXiv preprint arXiv:1804.02767*, 2018.

[40] O. Russakovsky, J. Deng, H. Su, J. Krause, S. Satheesh, S. Ma, Z. Huang, A. Karpathy, A. Khosla, M. Bernstein, A. C. Berg, and L. Fei-Fei. Imagenet large scale visual recognition challenge. *International Journal of Computer Vision*, 115(3):211–252, 2015.

[41] M. Sandler, A. Howard, M. Zhu, A. Zhmoginov, and L.-C. Chen. Mobilenetv2: Inverted residuals and linear bottlenecks. In *CVPR*, 2018.

[42] K. Simonyan and A. Zisserman. Very deep convolutional networks for large-scale image recognition. In *ICLR*, 2015.

[43] N. Srivastava, G. Hinton, A. Krizhevsky, I. Sutskever, and R. Salakhutdinov. Dropout: A simple way to prevent neural networks from overfitting. *Journal of Machine Learning Research*, 15:1929–1958, 2014.

[44] C. Szegedy, S. Ioffe, and V. Vanhoucke. Inception-v4, inception-resnet and the impact of residual connections on learning. In *ICLR Workshop*, 2016.

[45] C. Szegedy, W. Liu, Y. Jia, P. Sermanet, S. Reed, D. Anguelov, D. Erhan, V. Vanhoucke, and A. Rabinovich. Going deeper with convolutions. In *CVPR*, 2015.

[46] C. Szegedy, V. Vanhoucke, S. Ioffe, J. Shlens, and Z. Wojna. Rethinking the inception architecture for computer vision. In *CVPR*, 2016.

[47] M. Tan, B. Chen, R. Pang, V. Vasudevan, M. Sandler, A. Howard, and Q. V. Le. Mnasnet: Platform-aware neural architecture search for mobile. In *CVPR*, 2019.

[48] M. Tan and Q. V. Le. Efficientnet: Rethinking model scaling for convolutional neural networks. *arXiv preprint arXiv:1905.11946*, 2019.

[49] H. Touvron, A. Vedaldi, M. Douze, and H. Jégou. Fixing the train-test resolution discrepancy. In *NIPS*, 2019.

[50] A. Wan, X. Dai, P. Zhang, Z. He, Y. Tian, S. Xie, B. Wu, M. Yu, T. Xu, K. Chen, et al. Fbnetv2: Differentiable neural architecture search for spatial and channel dimensions. In *CVPR*, 2020.

[51] R. J. Wang, X. Li, and C. X. Ling. Pelee: A real-time object detection system on mobile devices. In *Advances in Neural Information Processing Systems*, pages 1963–1972, 2018.

[52] B. Wu, X. Dai, P. Zhang, Y. Wang, F. Sun, Y. Wu, Y. Tian, P. Vajda, Y. Jia, and K. Keutzer. Fbnet: Hardware-aware efficient convnet design via differentiable neural architecture search. In *CVPR*, 2019.

[53] S. Xie, R. Girshick, P. Dollár, Z. Tu, and K. He. Aggregated residual transformations for deep neural networks. In *CVPR*, 2017.

[54] S. Xie, A. Kirillov, R. Girshick, and K. He. Exploring randomly wired neural networks for image recognition. *ICCV*, 2019.

[55] Z. Yang, Z. Dai, R. Salakhutdinov, and W. W. Cohen. Breaking the softmax bottleneck: A high-rank rnn language model. In *ICLR*, 2018.

[56] X. Zhang, Z. Li, C. Change Loy, and D. Lin. Polynet: A pursuit of structural diversity in very deep networks. In *Proceedings of the IEEE Conference on Computer Vision and Pattern Recognition*, pages 718–726, 2017.

[57] X. Zhang, X. Zhou, M. Lin, and J. Sun. Shufflenet: An extremely efficient convolutional neural network for mobile devices. In *CVPR*, 2018.

[58] B. Zoph, V. Vasudevan, J. Shlens, and Q. V. Le. Learning transferable architectures for scalable image recognition. In *CVPR*, 2018.

Appendix

A Overview

This document presents further details and the additional experimental results of our proposed **Rank eXpansion Networks** (ReXNets). First, we show the validity of our training setup on ImageNet classification. It turns out that our training setup even shows better performance of MobileNetV1 [13] and MobileNetV2 [41] than those reported in the original papers (§B). Second, we provide the specifications of ReXNets, which are simple instance models according to our proposed design principles, yet they show prominent performances over diverse tasks as shown in the main paper (§C). Third, we provide extra experimental results including 1) model capacity comparison with EfficientNets [48] by training models from scratch on COCO dataset [25], 2) ReXNet with different nonlinear functions to justify choosing Swish-1 [36], and 3) model comparison with popular heavy models to show our models’ scalability (§D).

B ImageNet Classification Training Details

In this section, we first verify our training setup on ImageNet dataset [40] by comparing the scores between the officially reported ones and ours. Then, we provide further training details for ReXNets.

B.1 Training setup verification

We first verify our training setup in the paper with training MobileNetV2 [41] on ImageNet. This is because MobileNets [13, 41, 12] are challenging to reproduce with a few GPUs, it is crucial to show whether our training setup can reach the reported performance under a different environment³. We train with the network architectures which are officially released by the authors and report the accuracies. As shown in Table 7, our models seem to be trained well and even outperform the scores reported in the original papers [13, 41].

Table 7: **Training results of MobileNets.** MobileNets (ours) denote trained models with our training setup on ImageNet dataset [40] which are the identical architectures to the original ones [13, 41].

Network	Top-1 (%)	Top-5 (%)	MAdds	Params.
MobileNetV1 [13] (paper)	70.6	89.5	0.575B	4.2M
MobileNetV1 (ours)	72.5	90.7	0.575B	4.2M
MobileNetV2 [41] (paper)	72.0	91.0	0.300B	3.5M
MobileNetV2 (ours)	73.1	91.3	0.300B	3.5M

B.2 Further training details

Our models are trained using label smoothing [46] with the alpha of 0.1, dropout [43] rate of 0.2 on the last layer. As done in training the models of MobileNetV3 [12] and EfficientNet [48], we similarly train our models with stochastic depth [17] rate of 0.2, randaug [5] with the magnitude of 9, and random erasing [11] with the probability of 0.2.

³The original papers used 16 GPUs [41] or 4x4 TPU pods [12] for ImageNet training. We train all the models using 4 GPUs (V100 or P40).

Table 8: **Specification of ReXNet-1.0x**. Bottleneck1 and bottleneck6 denote the 3×3 inverted bottleneck with the expansion ratio of 1 and 6, respectively. In each block, SE denotes whether Squeeze Excitation Module (SE-module) [14] is used. SW denotes Swish-1 [36] is used after the convolution, and SW/RE6 denotes Swish and ReLU6 is used after the first 1×1 convolution and the 3×3 depthwise convolution [13], respectively.

Input	Operator	# of channels	SE	Nonlinearity	Stride
$224^2 \times 3$	conv 3×3	32	-	SW	2
$112^2 \times 32$	bottleneck1	16	-	SW/RE6	1
$112^2 \times 16$	bottleneck6	27	-	SW/RE6	2
$56^2 \times 27$	bottleneck6	38	-	SW/RE6	1
$56^2 \times 38$	bottleneck6	50	✓	SW/RE6	2
$28^2 \times 50$	bottleneck6	61	✓	SW/RE6	1
$28^2 \times 61$	bottleneck6	72	✓	SW/RE6	2
$14^2 \times 72$	bottleneck6	84	✓	SW/RE6	1
$14^2 \times 84$	bottleneck6	95	✓	SW/RE6	1
$14^2 \times 95$	bottleneck6	106	✓	SW/RE6	1
$14^2 \times 106$	bottleneck6	117	✓	SW/RE6	1
$14^2 \times 117$	bottleneck6	128	✓	SW/RE6	1
$14^2 \times 128$	bottleneck6	140	✓	SW/RE6	2
$7^2 \times 140$	bottleneck6	151	✓	SW/RE6	1
$7^2 \times 151$	bottleneck6	162	✓	SW/RE6	1
$7^2 \times 162$	bottleneck6	174	✓	SW/RE6	1
$7^2 \times 174$	bottleneck6	185	✓	SW/RE6	1
$7^2 \times 185$	conv 1×1 , pool 7×7	1280	-	SW	1
$1^2 \times 1280$	fc	1000	-	-	1

Table 9: **Specification of ReXNet_plain**. SW denotes Swish-1 is used after the convolution, and RE/SW denotes ReLU and Swish are used after the first 3×3 depthwise convolution and the following 1×1 convolution, respectively.

Input	Operator	# of channels	Nonlinearity	Stride
$224^2 \times 3$	conv 3×3	32	SW	2
$112^2 \times 32$	dwconv 3×3 / conv 1×1	96	RE/SW	2
$56^2 \times 96$	dwconv 3×3 / conv 1×1	144	RE/SW	1
$56^2 \times 144$	dwconv 3×3 / conv 1×1	192	RE/SW	2
$28^2 \times 192$	dwconv 3×3 / conv 1×1	240	RE/SW	1
$28^2 \times 240$	dwconv 3×3 / conv 1×1	288	RE/SW	2
$14^2 \times 288$	dwconv 3×3 / conv 1×1	336	RE/SW	1
$14^2 \times 336$	dwconv 3×3 / conv 1×1	384	RE/SW	1
$14^2 \times 384$	dwconv 3×3 / conv 1×1	432	RE/SW	1
$14^2 \times 432$	dwconv 3×3 / conv 1×1	480	RE/SW	1
$14^2 \times 480$	dwconv 3×3 / conv 1×1	528	RE/SW	1
$14^2 \times 528$	dwconv 3×3 / conv 1×1	576	RE/SW	2
$7^2 \times 576$	dwconv 3×3 / conv 1×1	624	RE/SW	1
$7^2 \times 624$	dwconv 3×3 / conv 1×1	1024	RE/SW	1
$7^2 \times 1024$	pool 7×7	1024	-	1
$1^2 \times 1024$	fc	1000	-	1

Note that we do not use FixResNet [49]-like techniques that need additional finetuning procedure after training. We do not use exponential moving average (EMA) used in training MobileNetV3 and EfficientNet. Training with the techniques may further improve the accuracy, so we will train our models with them as future work.

C Model Specifications of ReXNets

In this section, the detailed descriptions of ReXNets are presented. These models are simple instances of following our design principles of 1) expanding the input channel size, 2) replacing the nonlinearity of the expand layers, and 3) increasing the number of expand layers.

C.1 ReXNet

We do only a few changes in the layer configuration upon MobileNetV2 [41]. Specifically, we do not change the channel sizes of the stem (i.e., the first 3×3 convolution) and the penultimate layer (i.e., the last 1×1 convolution). We leave the original expansion ratio setting (each inverted bottleneck block has the ratio of 6 except for the first inverted bottleneck block that has the ratio of 1).

MobileNetV2 [41] has the channel sizes of each inverted bottleneck block of 32, 16, 24, 24, 32, 32, 32, 64, 64, 64, 64, 96, 96, 96, 160, 160, and 320, respectively. With the identical channel sizes of the stem (32) and the penultimate layer (1280), ReXNet has the following channel configuration: 32, 17, 27, 38, 50, 61, 72, 84, 95, 106, 117, 128, 140, 151, 162, 174, and 185 by expanding the input channel sizes and increasing the number of expand layers. We replace the ReLU6 at the expand layers in each inverted bottleneck block and the ReLU6 after the penultimate layer with Swish-1 [36]. We discard SE-modules [14, 12] in the inverted bottleneck blocks from the first to the bottleneck blocks with the stride 4 due to concerning the latency. The width multiplier is adopted to apply to all the channel sizes for scaling the model. The specification of ReXNet is shown in Table 8.

C.2 ReXNet_plain

A plain network such as MobileNetV1 [13] is able to be redesigned by following our design principles. Without changing the depth of MobileNetV1, we only redesign each channel and the nonlinearity of each convolution. MobileNetV1 has the channel sizes of each 1×1 convolution of 32, 64, 128, 128, 256, 256, 512, 512, 512, 512, 512, and 1024, respectively. We do slight modification on this to make many expand layers with expanded input channel size as 32, 96, 144, 192, 240, 288, 336, 384, 432, 480, 528, 576, and 624, respectively. All the other channel sizes including the stem and the output classifier are not changed. We only replace the ReLUs [33] after each 1×1 convolution to Swish-1, where the layer expand the channel size. We call this model ReXNet_plain. The specification of ReXNet_plain is shown in Table 9.

D Additional Experimental Results

D.1 Model capacity of ReXNets and EfficientNets

We further estimate the model capacity by **training the models from scratch** on COCO dataset [25]. This is to provide another experimental backup of the superior model capacity of ReXNets over EfficientNets not only on ImageNet classification but on COCO detection. We train ReXNets with the width multipliers from 0.9x to 1.3x in SSDLite, respectively and EfficientNets-B0, B1, and B2 in SSDLite, respectively. As shown in Table 10, ReXNets produce better AP scores than those of EfficientNets which show the consistent trend in Table 3 in the main paper. Therefore, we conclude that ReXNets have larger capacities for both finetuning and training from scratch.

Table 10: **Object detection results on COCO test-dev 2017.** We report the results of **training from scratch** on COCO train 2017 with ReXNets and EfficientNets in SSDLite.

Model	Input Size	Avg. Precision at IOU (%)			Params.	FLOPs
		AP	AP ₅₀	AP ₇₅		
EfficienNetB0 [48] + SSDLite	320x320	24.2	40.5	24.5	6.2M	0.97B
ReXNet-0.9x + SSDLite	320x320	24.9	41.4	25.4	5.0M	0.88B
ReXNet-1.0x + SSDLite	320x320	25.5	42.4	26.0	5.7M	1.01B
EfficienNetB1 [48] + SSDLite	320x320	25.9	42.7	26.3	8.7M	1.35B
ReXNet-1.1x + SSDLite	320x320	26.0	43.0	26.6	6.5M	1.19B
ReXNet-1.2x + SSDLite	320x320	26.3	43.5	26.9	7.4M	1.39B
EfficienNetB2 [48] + SSDLite	320x320	26.6	43.7	27.3	10.0M	1.55B
ReXNet-1.3x + SSDLite	320x320	26.8	44.1	27.4	8.4M	1.60B

D.2 ImageNet accuracy with different nonlinear functions

We studied how nonlinearity can affect the matrix rank of layers and model performance in the main paper. Here, we further study the actual impact of different nonlinear functions on model performance. We train ReXNet-1.0 with ELU [4], SoftPlus [6], LeakyReLU [30], and ReLU6 [41] to compare with the model with Swish-1 [36] on ImageNet. The result will provide the actual quality of the different nonlinearities. We obtain the results of top-1 accuracy which is better in the order of Swish-1 (77.90%), ELU (77.64%), SoftPlus (77.60%), Leaky ReLU (77.44%), and ReLU6 (77.26%) as shown in Table 11.

Table 11: **Trained ReXNet-1.0x with different nonlinear functions.** We verify the choice of nonlinearity in ReXNets by training the models with different nonlinear functions including ELU, Softplus, Leaky ReLU, and ReLU6 on ImageNet.

Network	Top-1 (%)	Top-5 (%)	FLOPs	Params.
ReXNet-1.0x with Swish-1 [36]	77.90	93.87	0.398B	4.80M
ReXNet-1.0x with ELU [4]	77.64	93.69	0.398B	4.80M
ReXNet-1.0x with Softplus [6]	77.60	93.75	0.398B	4.80M
ReXNet-1.0x with Leaky ReLU [30]	77.44	93.56	0.398B	4.80M
ReXNet-1.0x with ReLU6 [41]	77.26	93.49	0.398B	4.80M

D.3 Comparison with heavy models

We report the performances of ReXNet-2.0x and ReXNet-2.2x and other popular heavy models trained on ImageNet in Table 12. ReXNets show better performances over those of the reported heavy models with much less computational costs.

Table 12: **Heavy model comparison on ImageNet.** Our models are compared with popular models. Note that ReXNets are trained and evaluated with the fixed image size 224×224 .

Network	Top-1 (%)	Top-5 (%)	FLOPs	Params
VGG16BN [42]	71.5	89.8	15.5B	138.4M
VGG19BN [42]	74.2	91.8	19.7B	143.7M
ResNet18 [9]	69.8	89.1	1.9B	11.7M
ResNet50 [9]	76.1	92.9	4.1B	25.6M
ResNet101 [9]	77.4	93.6	7.9B	44.5M
ResNet152 [9]	78.3	94.1	11.6B	60.2M
InceptionV3 [46]	77.4	93.6	2.9B	27.2M
InceptionV4 [44]	80.0	95.0	13B	48M
Inception-ResNetV2 [44]	80.1	95.1	13B	56M
DenseNet169 [16]	76.2	93.1	3.4B	14.2M
DenseNet201 [16]	77.2	93.6	4.4B	20.0M
ResNeXt101_32x4d [53]	78.8	94.4	8.0B	44.2M
ResNeXt101_64x4d [53]	80.9	95.6	31.5B	83.6M
PolyNet [56]	81.3	95.8	34.7B	92.0M
RandWire-WS (C=109) [54]	79.0	94.4	4.0B	31.9M
EfficientNetB3 [48]	81.1	95.5	1.8B	12.2M
ReXNet-2.0x	81.6	95.7	1.5B	16.4M
ReXNet-2.2x	81.7	95.8	1.8B	19.4M